Production of the $K^0K^{\pm}\pi^{\mp}$ system in π^-p and K^-p interactions at 50, 100, and 175 GeV/c

C. Bromberg, J. O. Dickey, G. Fox, R. Gomez, W. Kropac, and S. R. Stampke
California Institute of Technology, Pasadena, California 91125

H. Haggerty and E. Malamud
Fermi National Accelerator Laboratory, Batavia, Illinois 60510

R. Abrams, R. Delzenero, H. Goldberg, F. Lopez,
S. Margulies, D. McLeod, and J. Solomon
University of Illinois at Chicago Circle, Chicago, Illinois 60680

A. Dzierba, F. Fredericksen, R. Heinz,
J. Krider, H. Martin, C. Peroni,
D. Petersen, and D. Zieminska
Indiana University, Bloomington, Indiana 47401
(Received 16 July 1984)

The reaction $\pi^-p \to K_S^0K^{\pm}\pi^{\mp}X$ has been studied at 50, 100, and 175 GeV/c. The observed $KK\pi$ effective-mass spectrum is well described by a model assuming longitudinal phase space and two-body resonances. Production of resonances in $K\pi$ and $K\bar{K}$ systems account for over 70% of the cross section. Estimated cross sections for $D(1285)$ and $E(1420)$ at 100 GeV/c are $\sigma_D B(D \to K^0K^{\pm}\pi^{\mp}) < 0.1$ μb and $\sigma_E B(E \to K^0K^{\pm}\pi^{\mp}) = 0.3 \pm 0.2$ μb. Results for the reaction $K^-p \to K_S^0K^{\pm}\pi^{\mp}X$ at 100 GeV/c are also presented.

I. INTRODUCTION

We present results of the analysis of the semi-inclusive production of the $K_S^0K^{\pm}\pi^{\mp}$ system at high energies. The data were collected as part of Fermilab experiment E110 using the Fermilab multiparticle spectrometer. The π^-p-induced data at beam momenta $P_{\rm inc}$ of 50 and 100 GeV/c, discussed in an earlier publication, indicated production of $D(1285)$ and $E(1420)$ resonances. In this paper, we present new data at $P_{\rm inc} = 175$ GeV/c. The reaction with an incident K^- instead of π^- is also discussed. We correct an error in the previous analysis due to the double counting of events, satisfying the K^* and δ cuts. We present a careful discussion of the background in the D- and E-meson mass range. We find that using a different background estimate leads to much smaller production cross sections of those resonances than reported in Ref. 1.

II. DATA SELECTION

The apparatus, event reconstruction, and selection criteria used to extract $\pi^-p \to K_S^0K^{\pm}\pi^{\mp}X$ data were described in detail in Ref. 1. The trigger was designed to select events with a neutral V and two charged particles, which trace back to the interaction vertex. An interaction in the target was demanded by requiring at least one hit in the cylindrical counters surrounding the target, thus suppressing events with a neutron as the only particle in the target fragmentation region. The identification of the charged particles from the interacting vertex was made using two Cherenkov counters. The momenta of both particles were required to be in the 6–45-GeV/c range where the differentiating power of the Cherenkov counters was sufficiently large. As a result of the above selection, we obtained 139, 2656, and 1069 events at the incident momenta 50, 100, and 175 GeV/c, respectively.

In the present study, we improved the momentum analysis which made some statistically insignificant changes in the D region. We applied a more stringent run selection

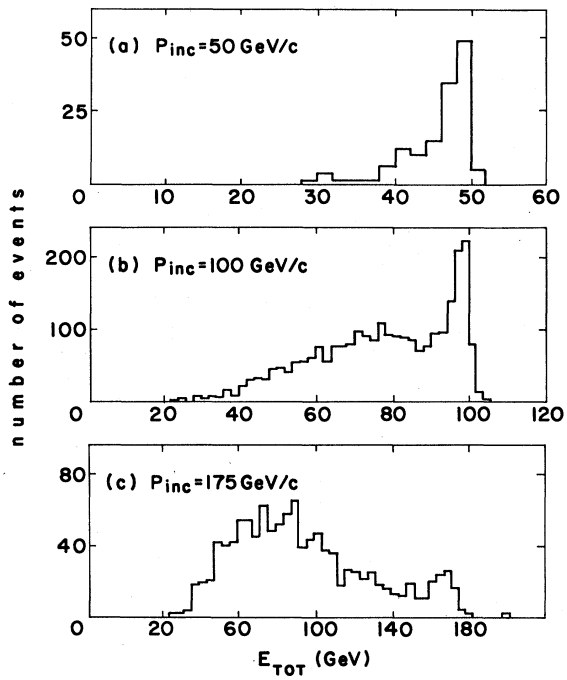

FIG. 1. Distributions of total energy of the $K^0K^{\pm}\pi^{\mp}$ systems in laboratory frame for reaction $\pi^- \to K^0K^{\pm}\pi^{\mp}X$ at (a) $P_{\rm inc} = 50$ GeV/c, (b) $P_{\rm inc} = 100$ GeV/c, and (c) $P_{\rm inc} = 175$ GeV/c.

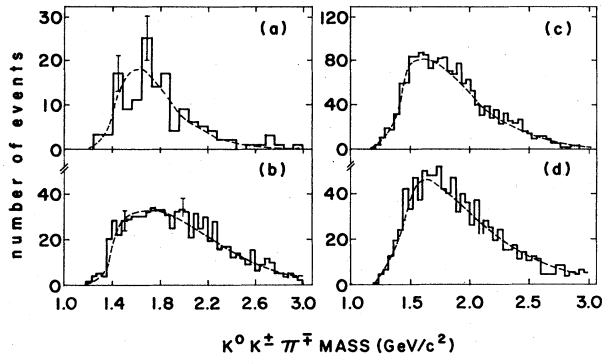

FIG. 2. Distributions of the invariant mass of the $K^0K^{\pm}\pi^{\mp}$ system produced in reaction $\pi^-p \rightarrow K^0K^{\pm}\pi^{\mp}X$ for (a) $P_{\text{inc}}=50$ GeV/c, (b) $P_{\text{inc}}=100$ GeV/c, $E_{\text{TOT}}>90$ GeV, (c) $P_{\text{inc}}=100$ GeV/c, $E_{\text{TOT}}<90$ GeV, and (d) $P_{\text{inc}}=175$ GeV/c. The curves are results of the seven-parameter fits described in the text.

which reduced the data sample by 15%. We would like to emphasize that none of our conclusions depend on those changes. The distribution of the total energy E_{TOT} carried by the $K^0K^{\pm}\pi^{\mp}$ system is shown in Fig. 1. At 50 GeV/c, the E_{TOT} spectrum is peaked near 50 GeV, thus showing that in most events there is no extra forward neutral particle in this case. The spectrum at 100 GeV/c has a narrow maximum near 100 GeV, corresponding to events with no forward neutral particles and a broad maximum at lower values of E_{TOT}, corresponding to events with at least one forward neutral particle. In the case of $P_{\text{inc}}=175$ GeV/c, the shape of the E_{TOT} spectrum indicates the presence of forward neutral particles in most events. In this analysis we will consider four separate samples: one at 50 GeV/c, two at $P_{\text{inc}}=100$ GeV/c, namely, 861 events with $E_{\text{TOT}}>90$ GeV and 1704 events with $E_{\text{TOT}}<90$ GeV, and one at $P_{\text{inc}}=175$ GeV/c, which we will denote by A, B, C, and D, respectively.

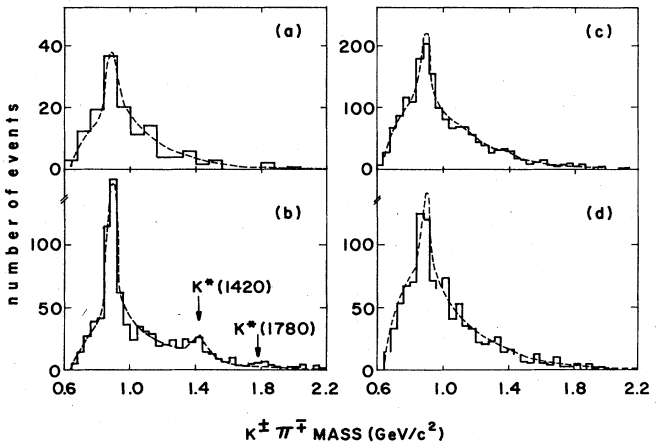

FIG. 3. Distributions of the invariant mass of the $K^{\pm}\pi^{\mp}$ system produced in reaction $\pi^-p \rightarrow K^0K^{\pm}\pi^{\mp}X$ for (a) $P_{\text{inc}}=50$ GeV/c, (b) $P_{\text{inc}}=100$ GeV/c, $E_{\text{TOT}}>90$ GeV, (c) $P_{\text{inc}}=100$ GeV/c, $E_{\text{TOT}}<90$ GeV, and (d) $P_{\text{inc}}=175$ GeV/c. The curves are results of the seven-parameter fits described in the text.

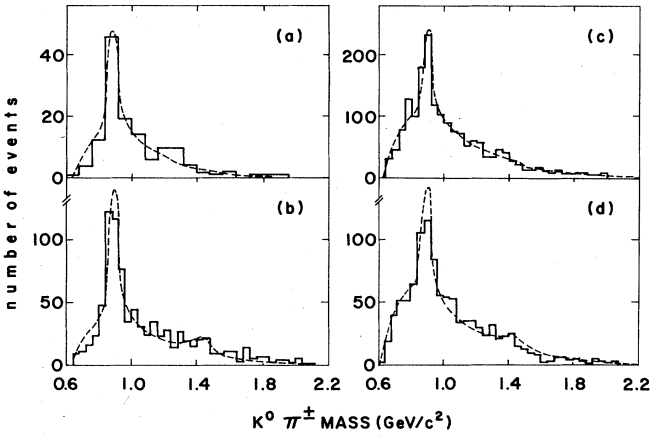

FIG. 4. Distributions of the invariant mass of the $K^0\pi^{\pm}$ system produced in reaction $\pi^-p \rightarrow K^0K^{\pm}\pi^{\mp}X$ for (a) $P_{\text{inc}}=50$ GeV/c, (b) $P_{\text{inc}}=100$ GeV/c, $E_{\text{TOT}}>90$ GeV, (c) $P_{\text{inc}}=100$ GeV/c, $E_{\text{TOT}}<90$ GeV, and (d) $P_{\text{inc}}=175$ GeV/c. The curves are results of the seven-parameter fits described in text.

III. BACKGROUND ESTIMATE

To find limits on the D- and E-meson production cross sections in the reaction

$$\pi^-p \rightarrow K^0K^{\pm}\pi^{\mp}X \ , \tag{1}$$

we consider two different approaches to the estimate of background.

The method used in Ref. 1 was based on deliberately misidentifying $\pi^{\pm}\pi^{\mp}K^0$ events as $K^{\pm}\pi^{\mp}K^0$ events by assigning the kaon mass to one of the pions. It was assumed that the $E(1420)$ meson undergoes predominantly quasi-two-body decays $E \rightarrow K^*\overline{K}$ and (or) $E \rightarrow \delta\pi$. The appropriate cross sections were found by requiring the $K\pi$ effective mass $M(K^{\pm}\pi^0)$ or $M(K^0\pi^{\pm})$ to be in the K^* region, or $M(KK)$ to be in the δ regions for both background events and the data, and subtracting one from the other in each case.

This method does not involve free parameters except for normalization. However, it neglects the fact that there are different two-body resonances involved in the two samples,

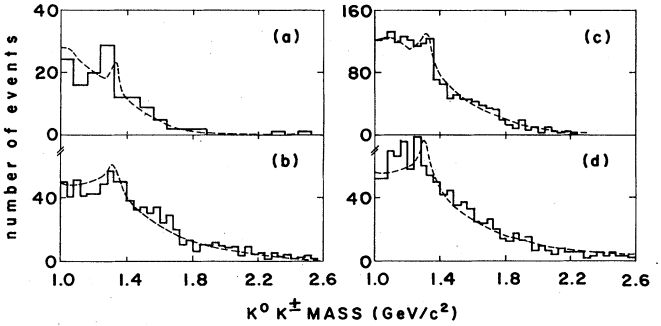

FIG. 5. Distributions of the invariant mass of the $K^0K^{\pm}$ system produced in reaction $\pi^-p \rightarrow K^0K^{\pm}\pi^{\mp}X$ for (a) $P_{\text{inc}}=50$ GeV/c, (b) $P_{\text{inc}}=100$ GeV/c, $E_{\text{TOT}}>90$ GeV, (c) $P_{\text{inc}}=100$ GeV/c, $E_{\text{TOT}}<90$ GeV, and (d) $P_{\text{inc}}=175$ GeV/c. The curves are results of the seven-parameter fits described in the text.

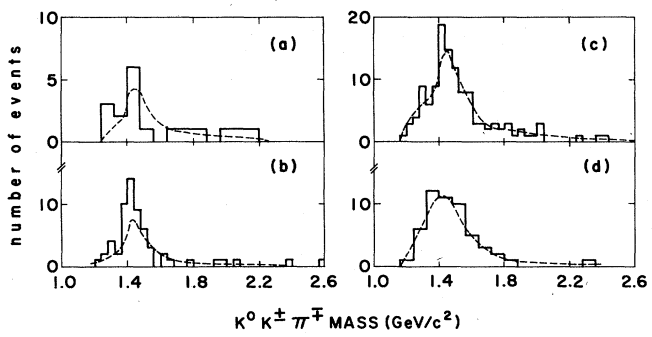

FIG. 6. Same as Fig. 2, with δ cut [$M(K^0K^\pm) < 1.04$ GeV/c^2].

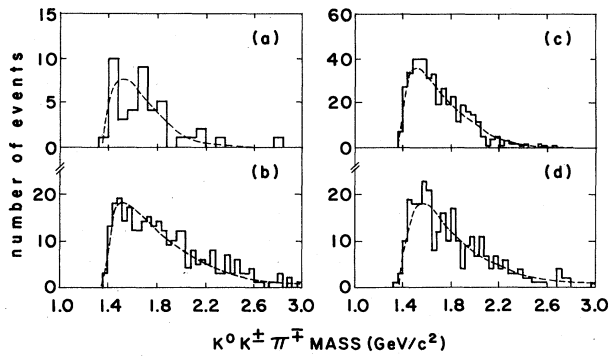

FIG. 7. Same as Fig. 2, with K^{*0} cut [$0.84 < M(K^\pm\pi^\mp) < 0.94$ GeV/c^2].

as well as the possible effect of a resonance structure of the $\pi\pi K$ spectrum. Moreover, different decay channels are treated independently in spite of a large overlap of the K^* and δ bands, leading to an overestimate of the total E-meson production cross section.

Another procedure to estimate contributions of various two- and three-body resonances is based on the maximum-likelihood method, as described in Refs. 2–4. Consider the matrix element squared of reaction (1) as a weighted sum of matrix elements squared $|M_i|^2$ of various channels, where the system $K^0K^\pm\pi^\mp$ is produced through the decay of intermediate systems: $K^*K, \delta\pi, A_2\pi$, etc. To obtain the appropriate fraction f_i, we search for a maximum of the likelihood function, defined as

$$L = \sum_{\text{events}} \ln \frac{\sum b_i^2 |M_i|^2}{\sum b_i^2 \int |M_i|^2 d\tau} \quad . \tag{2}$$

The sums in Eq. (2) extend over all channels. M_i denotes the matrix element for the channel i and b_i is the corresponding parameter to be fitted, while $d\tau$ denotes a phase-space element. The fractions f_i are related to the parameters b_i through the equation

$$f_i = \frac{b_i^2 \int |M_i|^2 d\tau}{\sum b_i^2 \int |M_i|^2 d\tau} \quad . \tag{3}$$

The matrix elements M_i are factorized into a longitudinal-phase-space part LPS common for all channels, and Breit-Wigner functions:

$$|M_i|^2 = \text{LPS} \times \text{BW}_i \quad . \tag{4}$$

For $K\pi$ and $K\bar{K}$ resonances, relativistic Breit-Wigner formulas were used, with energy-dependent widths and the mass and width parameters taken from Ref. 5. The $K\bar{K}_\pi$ resonances, D and E, were parametrized by the simple constant-width formula, with $M_D = 1.285$ GeV/c^2, $\Gamma_D = 0.026$ GeV/c^2, $M_E = 1.418$ GeV/c^2, and $\Gamma_E = 0.052$ GeV/c^2.

Events were generated according to the relativistically invariant phase space with a Gaussian distribution of transverse momentum of secondary particles.[6] For a given value of the incident momentum, we assumed the semi-inclusive reaction (1) to be well represented by the reaction

$$\pi^- p \rightarrow K_S^0 K^+ \pi^- (l\pi^0)(\pi^- p) \quad , \tag{5}$$

where $(\pi^- p)$ is the target-recoil system. The number of π^0 mesons was fixed, and set equal to 0, 1, or 2, as described below. We further imposed restrictions on particle momenta in accordance with experimental conditions.

In this method, the correct resonance structure is obtained in the two-body subchannels. However, one has to parametrize the production of resonances.

IV. RESULTS OF THE MAXIMUM-LIKELIHOOD ANALYSIS

In this section, we present experimental results for the four data sets A, B, C, and D. For each data set, we present the $KK\pi$ (Fig. 2), $K\pi$ (Figs. 3 and 4), and KK (Fig. 5) mass distributions, as well as the $KK\pi$ spectra for

TABLE I. Contributions to the $K^0K^\pm\pi K^\mp$ system.

Channel	Fraction (%) $\pi^- p \rightarrow K^0K^\pm\pi^\mp X$				$K^- p \rightarrow K^0K^\pm\pi^\mp X$
	A	B	C	D	
$K^{*\pm}(890)$	30 ±4	27 ±3	19 ±2	18 ±2	24 ±4
$K^{*0}(890)K^0$	21 ±3	30 ±3	14 ±2	13 ±2	16 ±3
$A_2(1320)\pi$	10 ±1	12 ±2	10 ±2	12 ±2	9 ±3
$K^{*\pm}(1430)$	1 ±4	4 ±2	1 ±1	3 ±1	1^{+3}_{-0}
$K^{*0}(1430)K^0$	1^{+3}_{-1}	6 ±1	1 ±1	1 ±1	0^{+2}_{-0}
$\delta(980)\pi$	9 ±2	4 ±1	3 ±1	2 ±1	0^{+2}_{-0}
$K_S^0K^\pm\pi^\mp$	25 ±6	13 ±5	50 ±4	50 ±4	44 ±8
$E \rightarrow K^*K$	0.1 ±0.1	0.0^{+1}_{-0}	1.3 ±0.6	0.1 ±0.7	1^{+2}_{-1}
$E \rightarrow \delta\pi$	$1.1^{+2}_{-1.1}$	3.2 ±2	1.1 ±0.6	1.1 ±0.6	0^{+2}_{-0}
$D \rightarrow \delta\pi$	1.7 ±1.7	$0.5^{+0.5}_{-0.2}$	0.6 ±0.4	0.2 ±0.4	1 ±1

TABLE II. Cross-section times branching ratio in μb.

Reaction	50 GeV/c	100 GeV/c	175 GeV/c
$\pi^- p \to E(1420)X$, $K^*K \to K^0K^\pm\pi^\mp$	< 0.1	$0.1 < \sigma < 0.3$	$0.02 < \sigma < 0.09$
$\pi^- p \to E(1420)X$, $\delta\pi \to K^0K^\pm\pi^\mp$	< 0.2	$0.1 < \sigma < 0.3$	< 0.03
$\pi^- p \to D(1285)X$, $\delta\pi \to K^0K^\pm\pi^\mp$	< 0.1	< 0.1	< 0.03

events with the KK effective mass in the δ region (Fig. 6) and, separately, for events with the $K^+\pi^-$ effective mass in the $K^*(890)$ region (Fig. 7).

The $K^0K^\pm\pi^\mp$ effective-mass distributions indicate possible production of the $E(1420)$ and $A_3(1680)$ resonances only in the case of $P_{\text{inc}} = 50$ GeV/c data in Fig. 2(a).

The $K\pi$ spectra are strongly dominated by the $K^*(890)$ resonance, especially in the cases where no additional forward particles are produced as seen in Figs. 3(a) and 3(b) and 4(a) and 4(b). In the $K^0K^\pm$ spectra, contributions from $\delta(980)$ and $A_2(1320)$ are seen.

The $K^0K^\pm\pi^\mp$ mass spectra with the KK system in the δ region are dominated by a large peak near 1.44 GeV/c^2. The position of the peak corresponds to the mass of the E meson.

The $K^0K^\pm\pi^\mp$ mass spectra for events, where the $K^\pm\pi^\mp$ mass is in the K^* region, $0.84 < M(K\pi) < 0.94$ GeV/c^2, are shown in Fig. 7. All spectra are peaked near K^*K threshold, although no clear indication for a resonant behavior is observed. A similar trend has been seen when $K^{*\pm}$ cuts were imposed.

For the maximum-likelihood analysis, we used the following set of parameters. We set the number of π^0 mesons in the final state, l, equal to 0 for data samples A and B, $l = 1$ for the data set C, and $l = 2$ for the $P_{\text{inc}} = 175$ GeV/c data. The parameter determining average transverse momenta squared of final particles has been varied between the values 0.16 and 0.25 (GeV/c)^2 so as to give the best agreement with the data. In all cases except B, the lower value has been used. In case B, we use the value 0.25 (GeV/c)^2. Final results for the relative contributions of various channels are not sensitive to this parameter. We consider two versions of the model. First, we include only two-meson resonances: $K^{*\pm}(890)$, $K^{*0}(890)$, $K^{*\pm}(1430)$, $K^{*0}(1430)$, $\delta(980)$, $A_2(1320)$, and a nonresonant term. This procedure involves altogether seven parameters. We then extend the procedure to include the D and E mesons, undergoing quasi-two-body decays: $D \to \delta\pi$, $E \to K^*K$, and $E \to \delta\pi$, bringing the number of parameters to ten.

The results of the seven-parameter fit are superimposed on the experimental histograms of Figs. 2–7. There is good agreement between the data and this simple model, based on the minimum dynamic assumptions.

Various intermediate states and their fitted relative contributions to the observed $K^0K^\pm\pi^\mp$ state are listed in Table I. The $K^*(890)K$ channels dominate, contributing up to 60%. The $\delta\pi$, $A_2(1320)\pi$, and $K^*(1430)K$ channels are also nonnegligible. The contributions from the D and E mesons are found rather small, the sum of their rates not exceeding 3%. We obtained the following numbers of D and E mesons produced at the three values of the incident momentum:

$$N_D = 2 \pm 2, \quad N_E = 2^{+5}_{-2} \text{ at } 50 \text{ GeV}/c ,$$

$$N_D = 14 \pm 8, \quad N_E = 68 \pm 30 \text{ at } 100 \text{ GeV}/c ,$$

and

$$N_D = 2^{+5}_{-2}, \quad N_E = 12 \pm 12 \text{ at } 175 \text{ GeV}/c .$$

A similar maximum-likelihood method has been applied to the reaction $K^- p \to K^0K^\pm\pi^\mp X$ at $P_{\text{inc}} = 100$ GeV/c. No significant signal of D and E mesons is observed. Results are given in Table I.

V. SUMMARY

We have studied the semi-inclusive reaction $\pi^- p \to K^0K^\pm\pi^\mp X$ at 50, 100, and 175 GeV/c. The observed $K^0K^\pm\pi^\mp$ mass spectrum covers the range between 1.14 and 3 GeV/c^2.

We applied two different methods of estimating background under the $D(1285)$ and $E(1420)$ resonances: one based on misidentifying $\pi^\pm\pi^\mp K^0$ events as $K^\pm\pi^\mp K^0$ events, the other based on simultaneous fit of various two-body resonances. Generally, the first method yields larger cross sections for the D- and E-resonance production. Treating results from the two methods as the upper and lower limits, we obtain the results summarized in Table II.

[1]C. Bromberg *et al.*, Phys. Rev. D **22**, 1513 (1980).
[2]S. J. Goldsack *et al.*, Nucl. Phys. **B29**, 529 (1971).
[3]J. Bartsch *et al.*, Nucl. Phys. **B46**, 356 (1972).
[4]A. Zieminski *et al.*, Nucl. Phys. **B69**, 502 (1973).
[5]Particle Data Group, Phys. Lett. **111B**, 1 (1982).
[6]D. C. Carey and D. Drijard, J. Comput. Phys. **28**, 327 (1978).